SELENE TRANSLUNAR TRAJECTORY RECONFIGURATION PLAN PROVIDED FOR THE CASE OF MAIN ENGINE ANOMALY

Yasuhiro Kawakatsu*

In this paper, the reconfiguration of translunar trajectory in case of main engine anomaly is investigated. The objectives of the trajectory design are to reduce the excessive velocity at the Lunar encounter as well as to reduce the total required Δv to complete the sequence. 3-impulse Hohmann transfer based trajectory is adopted and possible trajectories are categorized under 2-body approximation. The solutions obtained are applied to more sophisticated models (3-body approximation and 4-body) and yields feasible trajectory.

INTRODUCTION

SELENE is a Japanese Lunar explorer, which is planned to be launched in September, 2007 (Figure 1). SELENE is a Lunar polar orbiter of 100km altitude with two sub-satellites for gravity field measurement. The mission of SELELEN is to obtain the global scientific information of the Moon, which includes mapping of elemental abundance, mineralogical composition, topography and geological structure, and the gravity field data for both near and far side of the Moon with high accuracy and resolution. SELENE payload includes 14 instruments such as spectrometers and imagers. Synergistical analysis with these data will improve our understanding of the origin and evolution of the Moon.

Figure 2 shows the Lunar transfer sequence of SELENE. SELENE is once injected into a long elliptical phasing orbit around the earth, and after two rotations on the phasing orbit, it is injected into the translunar trajectory for the final approach to the Moon. At the Lunar encounter, a deceleration maneuver is performed at the perilune passage of the Lunar approaching hyperbolic orbit, and SELENE is injected into a Lunar orbit.

Figure 1 Overview of SELENE

* Institute of Space and Astronautical Science, Japan Aerospace Exploration Agency
3-1-1 Yoshinodai, Sagamihara, Kanagawa, 229-8510, Japan E-mail: Kawakatsu.Yasuhiro@jaxa.jp

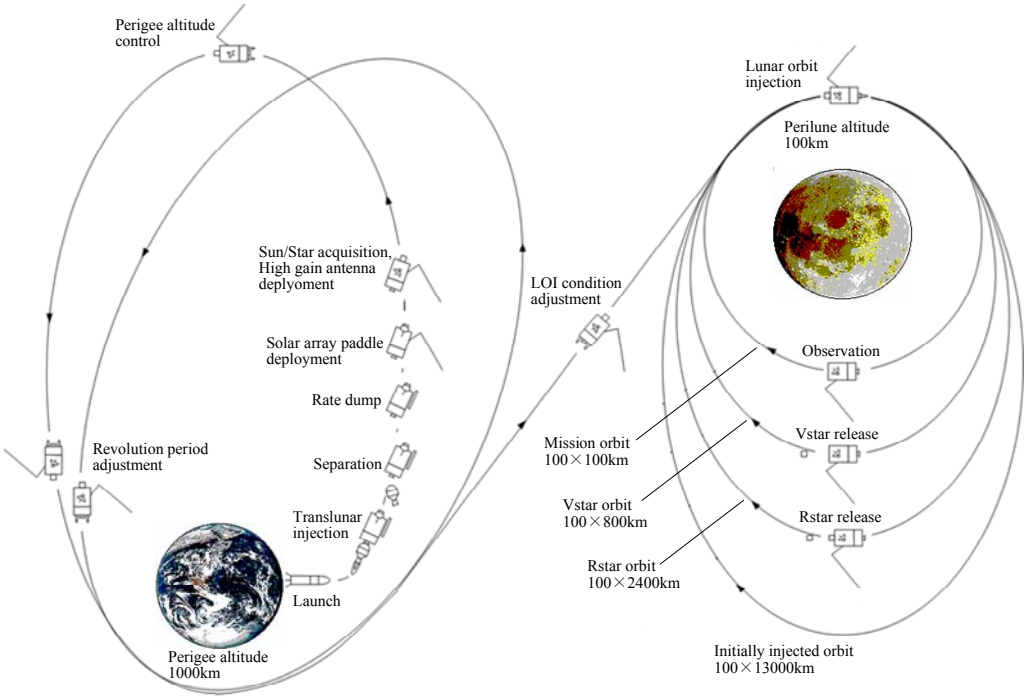

Figure 2 SELENE Lunar Transfer Sequence

The Lunar orbit injection maneuver is planned to be performed by a 500N bi-propellant main engine. It is the only large thrust engine onboard, and the remaining way to produce effective axial thrust is to use twelve 20N mono-propellant thrusters, which are originally planned to be used for the attitude control during the main engine maneuver and small orbit maneuvers during the operation.

A situation discussed in this paper is that, it turns out prior to the Lunar orbit injection that the main engine is unable to be used. The situation supposes not only faults in the main engine, but also other obstacles such as the misalignment of the main engine thrust axis and the spacecraft's mass center due to the solar array paddle deployment failure, or the double failure on the 20N thrusters in the same control direction. It must be noted that, in any case, the situation is “contingency”, which is not caused by a single fault, and the possibility of the emergence of the anomaly is extremely low.

The problems in this case are summarized as the following two points. Firstly, the main engine is the only bi-propellant engine on board. Its unavailability makes the oxidizer useless and the substitution by the mono-propellant thruster lower the specific impulse of the maneuver. As a result, the total Δv attainable is reduced and it becomes impossible to reach the originally planned mission orbit (that is, a circular orbit with the altitude 100km.) Secondly, there is a restriction in the continuous operation time of the 20N thrusters, which limits the Δv attainable by a single maneuver to be less than approximately 100m/s. On the other hand, the original lunar encounter condition requires more than 200m/s of Δv to be captured by the Moon.

To cope with this situation, a trajectory reconfiguration plan is investigated. The primary objective of the trajectory reconfiguration is to reduce the excessive velocity at the lunar encounter to lower the minimum required Δv to be captured by the moon. The second objective is to reduce the total required Δv to complete the sequence, so as to enable the improvement of the observation condition or the enhancement of the operation life.

In the scope of the paper, the anomaly is supposed to be detected sufficiently early so that the lunar encounter condition is able to be modified by a moderate correction maneuver in advance. It is assumed that the anomaly is detected before the final trajectory correction maneuver planned at 3 days before LOI (it is approximately 2 weeks from the launch). Since some maneuver operations (using the main engine) are planned prior to this maneuver, if any problem, it is likely to be detected prior to this time limit.

The basic concept of the reconfigured trajectory is described as follows (The number coincides with the notation in Figure 3).

1. Main engine anomaly is detected on the way to the Moon of the original trajectory.
2. Correction maneuver is performed to modify the lunar encounter condition.
3. SELENE flies by the moon and swung out to a distant apogee by the gravity assist of the Moon.
4. Deep space maneuver (DSM) is performed nearby the apogee to adjust the orbit to re-encounter the Moon.
5. SELENE re-encounters the Moon.

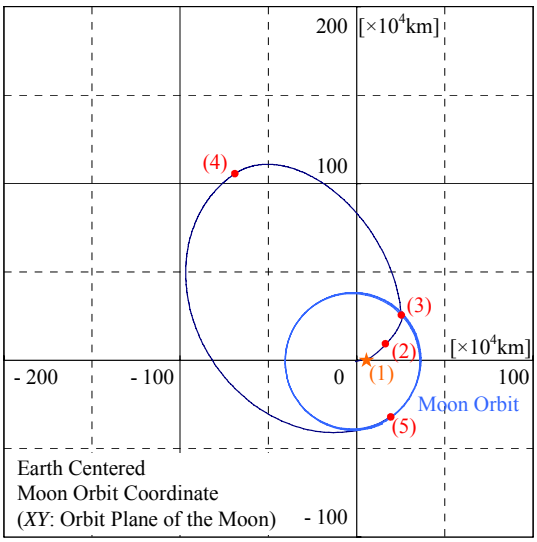

Figure 3 Basic Concept of the Reconfigured Trajectory

By carefully tuning the first Lunar encounter condition, the amount of DSM and the excessive velocity (v_∞) at the re-encounter can be reduced sufficiently. In addition, if the geometric relation between the trajectory and the Sun is desirable, the perturbation by the Sun gravity can be applied effectively, which results in the further reduction of the DSM.

This concept is basically the same as the sequence proposed by Belbruno and Miller (Ref. 7 and 8) or Yamakawa (Ref. 9 and 10). However, there is a small but an important difference in case of SELENE, that the condition of the first lunar encounter is strongly constrained by the original nominal translunar trajectory. Basically, the position and the time of the first lunar encounter cannot be shifted widely from those of the original condition. In the previous works, the encounter condition was important design parameters, because it determines the geometric relation between the trajectory and the Sun, which closely related to the effective application of the perturbation by the Sun gravity. Therefore, the constraint in the first lunar encounter condition in the case of SELENE means that the way to control the effect of the perturbation by the sun gravity is strongly restricted.

Under this situation, to widen the design flexibility and to find a better (less Δv) solution, wider range of the trajectory configurations are considered in this work. All of the trajectory configurations conserve essential features of the basic concept shown in Figure 3. That is, the time of the Lunar swing-by (t_{LSB}), the inclusion of one lunar swing-by and one DSM, and small v_∞ at the Lunar re-encounter ($v_{\infty LRE}$). On the other hand, the trajectory configurations differ in the remaining features, such as the time of DSM (t_{DSM}), the time of the Lunar re-encounter (t_{LRE}), and the number of rotations before and after DSM. Therefore, the effect of the perturbation by the sun gravity differs by the trajectory configurations even though their start point are the same (that is, the constraint in the first lunar encounter condition in the case of SELENE is satisfied.)

Various configurations of the trajectories are initially designed under 2-body approximation based on the concept of 3-impulse Hohmann transfer. By using the trajectories obtained under 2-body approximation, the detailed trajectories are designed under the 3-body and 4-body approximation. The design parameters, such as the swing-by condition at the first lunar encounter, t_{DSM} and t_{LRE}, are tuned and Δv at DSM (Δv_{DSM}) and $v_{\infty LRE}$ are estimated for each trajectories. The performance of the trajectory differs by the trajectories depending on the effect of the perturbation by the Sun gravity during the sequence. The trajectory with the better performance is selected as the candidate of the reconfigured trajectory.

In the following sections, the trajectory design process is introduced step by step with the examples of the designed trajectories.

TRAJECTORY DESIGN PROCESS

Two body problem approximated solutions

The concept of the reconfigured trajectory introduced in the previous section is based on the 3-impulse Hohmann transfer. Figure 4 depicts the concept of 2-impulse and 3-impulse Hohmann transfer. It is known that, when $r_2/r_1 > 15.58$, for arbitrary selection of $r_m(> r_2)$, total Δv required for 3-impulse Hohmann transfer is smaller than that required for 2-impulse Hohmann transfer. Here, r_1, r_2 and r_m denotes the radius of the initial orbit, the terminal orbit and the intermediate apogee respectively. In case of the Lunar transfer, the ratio r_2/r_1 is approximately 60, and it is in the range where 3-impulse Hohmann transfer is the superior. Additionally, there are two features of this problem which may give advantage to 3-impulse Hohmann transfer. Firstly, by the usage of the Lunar swing-by, Δv to inject from the initial orbit to the transfer orbit (Δv_1) can be reduced compared to the case of direct transfer to the intermediate apogee. Secondly, if the geometric relation between the trajectory and the Sun is desirable, the perturbation by the Sun gravity could be utilized effectively to reduce Δv at intermediate apogee (Δv_2) or Δv to inject from the transfer orbit to the final orbit (Δv_3).

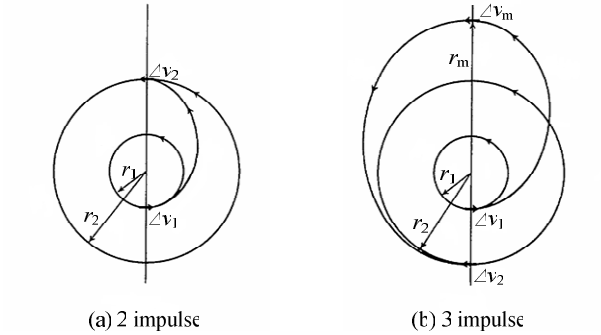

(a) 2 impulse (b) 3 impulse

Figure 4 2 Impulse and 3 Impulse Hohmann Transfer

Based on the concept of 3-impulse Hohmann transfer, the trajectory (from the Lunar swing-by) to transfer to the orbit of the Moon is designed by the following procedure (Figure 5).

1. The time of the Lunar swing-by (t_{LSB}) and v_∞ at the Lunar swing-by ($v_{\infty LSB}$) are given from the Lunar encounter condition of the nominal trajectory. By setting the azimuth and the elevation of v_∞ after the Lunar swing-by (α_{LSB} , δ_{LSB} respectively), the trajectory after the Lunar swing-by is determined (green line in Figure 5). α_{LSB} is the angle between $v_{\infty LSB}$ after the Lunar swing-by and the velocity of the Moon measured within the orbit plane of the Moon, and δ_{LSB} is the angle between $v_{\infty LSB}$ after the Lunar swing-by and the orbit plane of the Moon. δ_{LSB} is constantly set to 0 (i.e. the trajectory after the Lunar swing-by is limited in the orbit plane of the Moon), and α_{LSB} is restricted so as the perilune radius at the Lunar swing-by to be larger than the radius of the Moon.
2. At the apogee of the trajectory after the Lunar swing-by, a deep space maneuver (DSM) is performed in tangential direction (the time of DSM (t_{DSM}) is determined). Δv at DSM (Δv_{DSM}) is determined so that the trajectory after DSM (orange line in Figure 5) tangent at its perigee to the orbit of the Moon.
3. At the perigee of the trajectory after DSM, SELENE arrives at the orbit of the Moon (blue point in Figure 5). The angle at the arrival and the phase angle (θ) at the arrival are determined. θ is the angle from the perigee direction of the Moon measured within the orbit plane of the Moon.

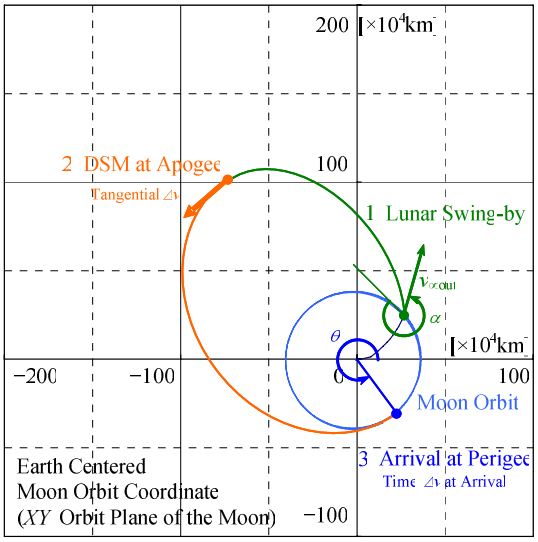

Figure 5 Trajectory Design to Transfer to the Moon Orbit (2-Body Approximation)

Obviously, designed by the procedure above is the trajectory to transfer to the orbit of the Moon, and the re-encounter with the Moon is not guaranteed for the designed trajectory. The trajectory to re-encounter with the Moon can be selected from the designed trajectories in the following way (Figure 6). Firstly, the plots in dark blue of Figure 6 denote the sets of the time and θ at the terminal (i.e. arrival at the orbit of the Moon) of the trajectories designed in the procedure above for various α_{LSB} . Though it seems intermittent plots in the right hand side region due to the discrete α_{LSB} , essentially it is consistent line. Two lines (upper and lower) are observed in the figure. The upper line is the plots of the trajectory which goes out-bounds of the orbit of the Moon just after the Lunar swing-by (Figure 7 (a)). The lower line is the plots of the trajectory which goes in-bounds of the orbit of the Moon just after the Lunar swing-by (Figure 7 (b)). Next, the plots in light blue of Figure 6 denote the sets of the time and θ of the Moon. Then, the intersection of the dark and the light blue lines (marked by red circles) means that SELENE and the Moon is at the same place at the same time, namely, the re-encounter.

Each intersection (marked with red circle) in Figure 6 denotes individual trajectory that re-encounter with the Moon. The labels (ex. *out_0*) denotes the direction of the trajectory (out-bounds or in-bounds) and the number of the rotation of the Moon from the swing-by to the re-encounter (the integer after the underscore). Figure 7 shows the trajectories that re-encounter with the Moon selected in Figure 6. Five out-bounds trajectories and four in-bounds trajectories are shown in the figure.

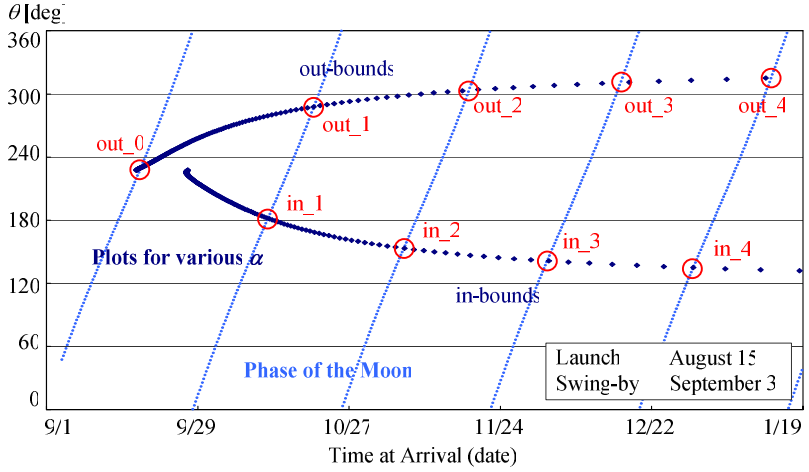

Figure 6 Selection of the Trajectory to Re-encounter the Moon

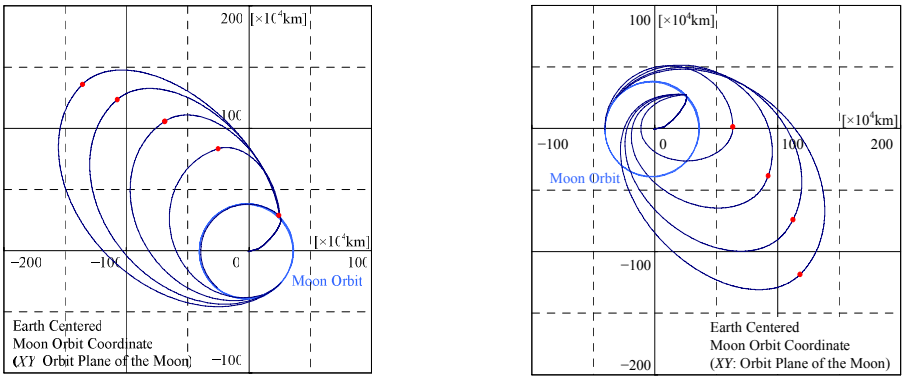

(a) Out-bounds trajectories (b) In-bounds trajectories

Figure 7 Designed Trajectories to Re-encounter the Moon

The trajectories shown in Figure 7 are the typical set of the trajectories based on the concept of 3-impulse Hohmann transfer, however, they are not all of them. Other series of "3-impulse Hohmann transfer based trajectories" can be constructed by increasing the number of rotations (around the Earth) before and after DSM. In the case of trajectories shown in Figure 7, the numbers of rotations before and after DSM are both 0. Figure 8 shows three examples of the other trajectory configurations. It can be seen that the number of rotations in the trajectory before DSM (green line) and the trajectory after DSM (orange line) are different in the three examples.

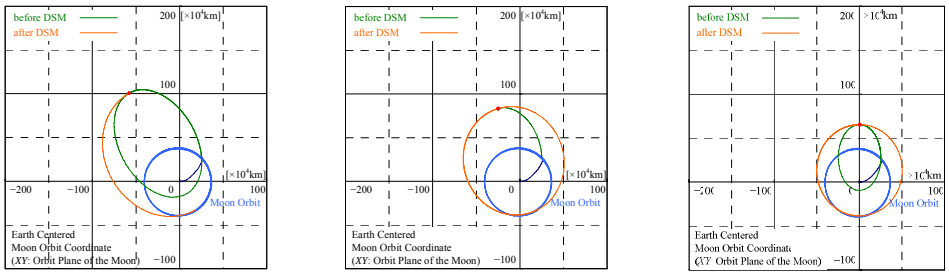

(a) 1 rotation before DSM (b) 1 rotation after DSM (c) 1 rotation before DSM 1 rotation after DSM

Figure 8 Expansion of Possible Trajectories under 2-Body Approximation

Considering the various configurations of the trajectories (i.e. the number of rotations before and after DSM), much more possible trajectories are obtained to re-encounter with the Moon. Figure 9 is the same plot as Figure 6, but includes more plots of various configurations of the trajectory. Many intersections of the dark and the light blue lines denote the possible trajectories that re-encounter with the Moon. Considering the conditions related to the practical operation below, 19 feasible trajectories (marked in red solid circle in Figure 9) are selected from the possible trajectories (the unselected trajectories are marked in blue cross in Figure 9). The conditions considered are,

- Distance at DSM < 2,000,000km.
- Δv_{DSM} < 300m/s.
- t_{LRE} < t_{LSB} + 4 months
- $v_{\infty LRE}$ < 300m/s

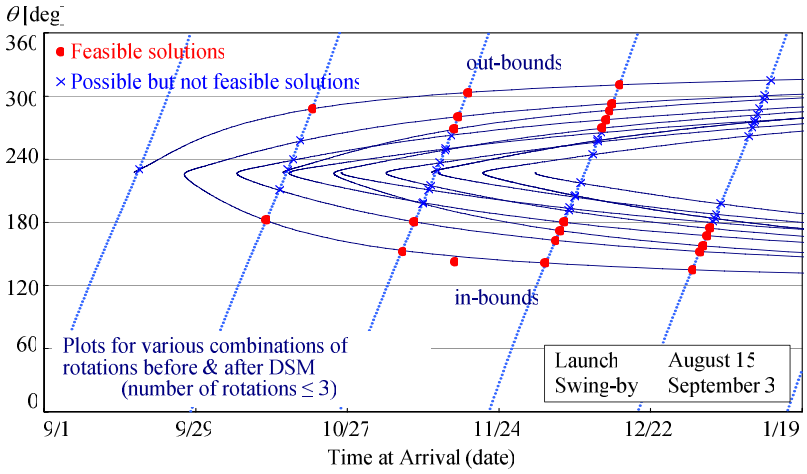

Figure 9 Possible Solutions under 2-Body Approximation

Figure 10 shows the 19 feasible trajectories selected in Figure 9. The labels (ex. *00_out_0*) denotes the number of rotations before and after DSM (the two integer before the first underscore), the direction of the trajectory (out-bounds or in-bounds), and the number of the rotation of the Moon from the swing-by to the re-encounter (the integer after the second underscore).

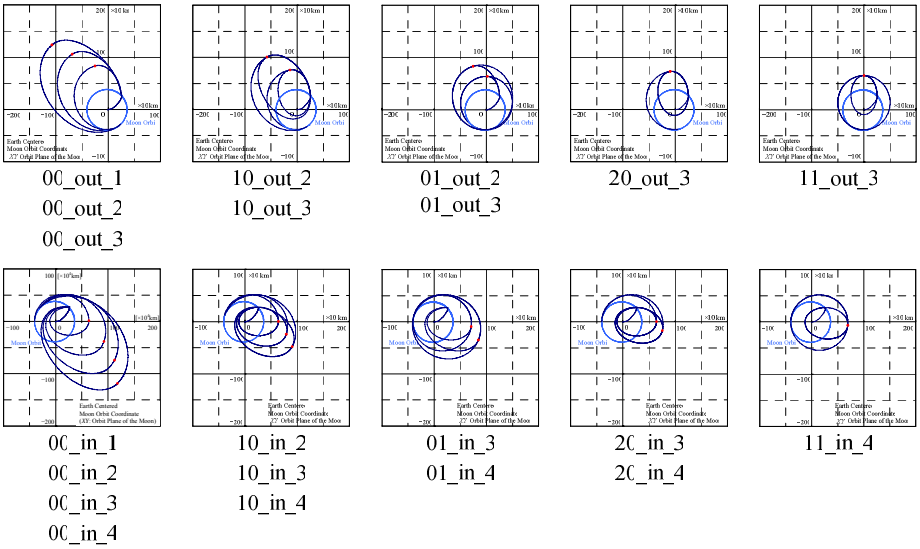

Figure 10 Possible Trajectories under 2-Body Approximation

Trajectory Design under 3-Body Approximation

Following the results of the investigation under 2-body approximation, the trajectory design is performed taking into account the perturbation by the Sun gravity. Namely, it is the trajectory design under 3-body approximation. The consideration of the Sun gravity makes possible to assess if the perturbation by the Sun gravity can be utilized effectively to reduce Δv_{DSM} and $v_{\infty LRE}$. Naturally, the effect of the perturbation strongly depends on the geometric relation between the trajectory and the Sun. Therefore, it is expected that the effect differs by the trajectories shown in Figure 10.

The trajectories are designed based on the results under 2-body approximation. As to the four parameters, α_{LSB}, δ_{LSB}, t_{DSM} and t_{LRE}, the values obtained under 2-body approximation are used as they are in the trajectory design under 3-body approximation. And Δv_{DSM} is tuned to target the final position of the trajectory (i.e. the position of the Moon at t_{LRE}), so that the closed trajectory is obtained under 3-body approximation.

This procedure is applied to the 21 possible trajectories obtained under 2-body approximation, however, not all the cases give the expected designed trajectory under 3-body approximation.

For 6 cases,

00_in_1, *00_in_4*, *00_out_1*, *00_out_2*, *01_out_2*, *01_out_3*

the designed trajectory converged to the configuration as expected. The numbers of rotations before/after DSM in the obtained trajectory hold the numbers in the respective original trajectory obtained under 2-body approximation. Figure 11 shows the two examples in this category (*00_out_1* and *01_out_2*), in which the trajectory obtained under 2-body approximation (blue line) and that obtained under 3-body approximation (red line) are drawn in the same figure. It is observed that the shape of the trajectory transformed by the perturbation of the Sun gravity, however, the configuration of the trajectory (i.e. the numbers of rotations before/after DSM) is remain unchanged in the trajectory obtained under 3-body approximation.

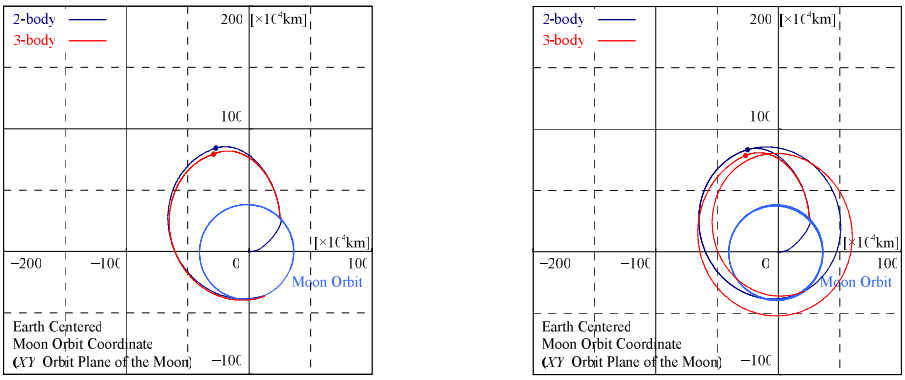

(a) 00_out_1 (b) 01_out_2

Figure 11 Cases that 2-Body Solutions Give Good Initial Estimation

For the other 15 cases, the designed trajectory does not converged to the configuration as expected. In some cases, the targeting process is converged (that is, Δv_{DSM} to satisfy the terminal position is obtained), however, the configuration of the designed trajectory is not the same as that of the original trajectory obtained under 2-body approximation. In other cases, the targeting process is not converged and the closed trajectory is not obtained under 3-body approximation. Two reasons are supposed to explain the situation of these 15 cases. First is that, the value of the four parameters inherited from the results of the 2-body approximation is inappropriate for the trajectory design under 3-body approximation. Second is that, the geometric relation between the trajectory and the Sun is inappropriate, so that the perturbation by the Sun gravity effects in undesirable way. At this moment, the detail is under investigation.

In the design above, the values of four parameters are fixed to the values inherited from the results under 2-body approximation. Naturally, those values are not optimized for the trajectories under 3-body approximation and there remains the space for improvement. In other words, it is possible to reduce the total Δv required to complete the sequence by tuning the value of these parameters.

Four parameters, α_{LSB}, β_{LSB}, t_{DSM} and t_{LRE} are tuned to minimize the specific Δv (Δv_{sp}) defined as

$$\Delta v_{sp} = \Delta v_{DSM} + \Delta v_{LOI} \qquad (1)$$

where Δv_{LOI} is Δv required for the Lunar orbit injection, calculated from $v_{\infty LRE}$ assuming the injection into the Lunar orbit of perilune radius 1838km and apolune radius 30000km. In each step of the optimization (i.e. whenever the parameters are updated), Δv_{DSM} is tuned to target the final position of the trajectory (i.e. the position of the Moon at t_{LRE}), so that the closed trajectory is obtained.

This optimization procedure is applied to the 4 cases (*00_in_1*, *00_out_1*, *00_out_2*, and *01_out_3*) which give the expected designed trajectory in the previous step. The result of the optimization is summarized in Table 1. It is observed that the shape of the optimized trajectory (red line) transformed from that before the optimization (blue line), however, the configuration of the trajectory (i.e. the numbers of rotations before/after DSM) is remain unchanged in the trajectory after optimization. The value of performance index Δv_{sp} is improved largely as a result of the optimization. The quantity of the reduction depends on the cases. The order of the Δv_{sp} among the four cases seems unchanged between "before" and "after" the optimization, however, it is questionable that this rule can be applied in general. More moderate rule (ex. "There is a tendency that …) may be possible, however, further investigation is required for this point. Additionally, it must be noted that the Δv_{LOI} required for the first Lunar encounter is estimated approximately as 210m/s. Δv_{sp} of *00_out_1*, *00_out_2*, and *01_out_3* are smaller than this value, and it means that the total required Δv to complete the sequence is reduced at this step of 3-body approximation.

Table 1 Results of the Parameter Optimization
($^{(*)}\Delta v_{sp\_0}$ denotes Δv_{sp} before optimization)

	00_in_1	00_out_1	00_out_2	01_out_3
$(\Delta v_{sp\_0})^{(*)}$	(420.3m/s)	(178.9m/s)	(356.9m/s)	(281.9m/s)
Δv_{sp}	283.8m/s	106.8m/s	183.3m/s	120.7m/s
Δv_{DSM}	86.4m/s	1.0m/s	108.9m/s	46.5m/s
Δv_{LOI}	197.4m/s	105.8m/s	74.4m/s	74.2m/s
Trajectory	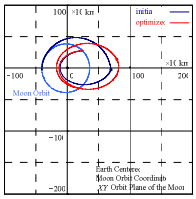	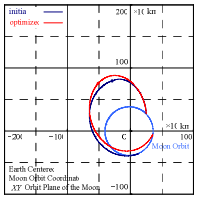	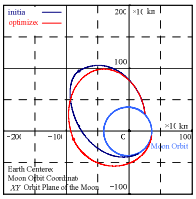	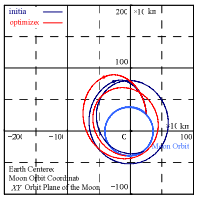

Trajectory Design under 4-Body Approximation

Following the results of the investigation under 3-body approximation, the trajectory design is performed taking into account the perturbation by the Lunar gravity. Namely, it is the trajectory design under 4-body approximation. The consideration of the Lunar gravity refines the orbit dynamics modeling at the Lunar swing-by and the Lunar re-encounter and it enables more practical Δv estimation. The Δv at the maneuver prior to the Lunar swing-by to adjust the Lunar swing-by condition (Δv_{adj}) is calculated, and the third body (i.e. the Earth) effect at the Lunar re-encounter is reflected on the value of Δv_{LOI}.

The trajectories are designed based on the results under 3-body approximation. As to the five parameters, $\boldsymbol{r}_{DSM}$ (include 3 components), t_{DSM} and t_{LRE}, the values obtained under 3-body approximation are used as they are in the trajectory design under 4-body approximation. Δv_{adj} is tuned to target $\boldsymbol{r}_{DSM}$ and Δv_{DSM} is tuned to target the final condition of the trajectory, so that the closed trajectory is obtained under 4-body approximation. The final condition is defined on the Moon-fixed coordinate system at t_{LRE}. The inclination, the radius, and the true anomaly are assigned to 90deg., 1838km, and 0deg. respectively.

This procedure is applied to the case *00_out_1*, which gives the smallest Δv_{sp} as a result of the optimization process under 3-body approximation. Figure 13 shows the result of the trajectory design under 4-body approximation. Drawn in the figure are the trajectories obtained under 3-body approximation (blue line) and that obtained under 4-body approximation (red line). It is observed that the transformation of the trajectory from 3-body to 4-body is smaller than that from 2-body to 3-body. It can be concluded that the value of the five parameters inherited from the results of the 3-body approximation is sufficiently effective as initial estimates under 4-body approximation. Figure 14 shows the sequence of events of the reconfigured trajectory denoted on the trajectory designed under 4-body approximation. After the main engine anomaly is detected on the way to the Moon, 39.0m/s of adjust maneuver is performed on August 31 (approximately 3 days before the Lunar swing-by). SELENE flies by the Moon on September 3 and 64.0m/s of DSM is performed on September 28 at the 900,000km distant from the Earth. SELENE re-encounters the Moon on October 24 and injected into the Lunar orbit of perilune radius 1838km and apolune radius 30000km by 116.1m/s of LOI maneuver. Though the value of Δv_{LOI} is slightly larger than the target value (less than 100m/s approximately), it seems adjustable by enlarging the apolune altitude if necessary. From this result, it can be concluded that the feasible reconfigured trajectory is obtained.

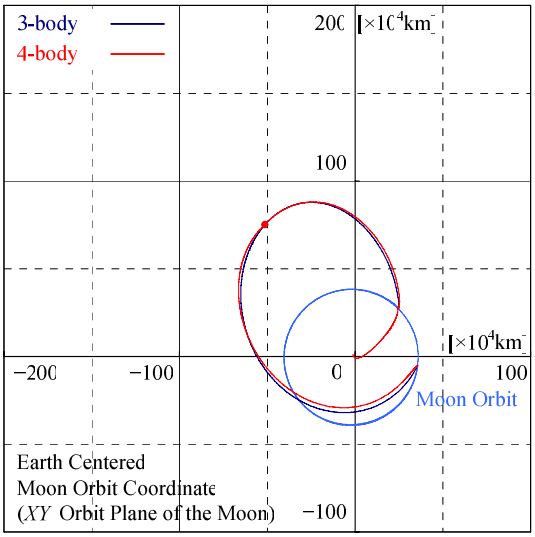

Figure 13 Results of the Design under 4-body approximation

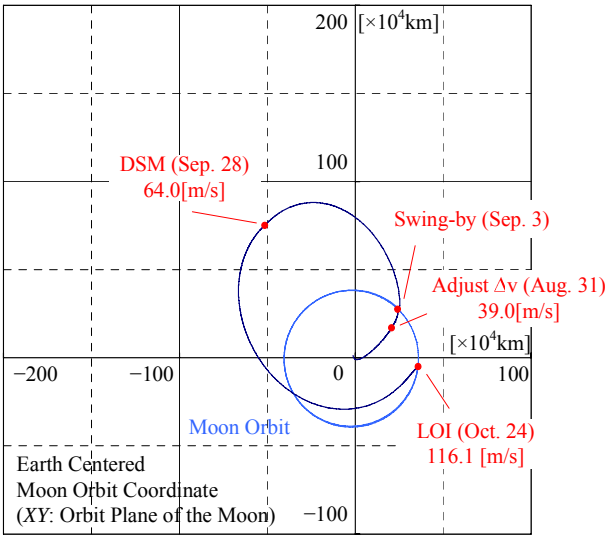

Figure 14 Example Sequence of Reconfigured Trajectory

The value of Δv_{DSM} and Δv_{LOI} obtained under 4-body approximation is larger than those listed on Table 1, the results of the optimization process under 3-body approximation. The reason is that, the values of five parameters are fixed to the values inherited from the results under 3-body approximation. Naturally, those values are not optimized for the trajectories under 4-body approximation and there remains the space for improvement. In other words, it is possible to reduce the total Δv required to complete the sequence by tuning the value of these parameters. It remains for further investigation.

CONCLUSION

In this paper, the reconfiguration of translunar trajectory in case of main engine anomaly is investigated. The objectives of the trajectory design are to reduce the excessive velocity at the lunar encounter as well as to reduce the total required Δv to complete the sequence. 3 impulse Hohmann transfer based trajectory is adopted and possible trajectories are categorized under 2-body approximation. The solutions obtained are applied to more sophisticated models (3-body approximation and 4-body) and yields feasible trajectory.

LIST OF SYMBOLS AND ABBREVIATIONS

DSM	Deep space maneuver
LOI	Lunar orbit injection
Δv	Velocity increment
v_∞	Excessive velocity
Δv_{sp}	Specific Δv (performance index for trajectory optimization)
Δv_{adj}	Δv to adjust the Lunar swing-by condition
Δv_{DSM}	Δv at DSM
Δv_{LOI}	Δv at LOI
$v_{\infty LSB}$	v_∞ at Lunar swing-by
$v_{\infty LRE}$	v_∞ at Lunar re-encounter
α_{LSB}	Azimuth of v_∞ after Lunar swing-by
δ_{LSB}	Elevation of v_∞ after Lunar swing-by
t_{DSM}	Time of DSM
t_{LRE}	Time of Lunar re-encounter
t_{LSB}	Time of Lunar swing-by
θ	Phase angle on the orbit of the Moon

REFERENCES

1. Kawakatsu Y., Kaneko Y., Takizawa Y., Design of Translunar Trajectory and Relay Satellite Orbit of SELENE, *Proceedings of the 21st International Symposium on Space Technology and Science*, 1998.
2. Kawakatsu Y., Nakajima K., Ogasawara M., et al., SELENE Translunar Trajectory and Luanr Orbit Injection, *Proceedings of the 14th International Symposium on Space Flight Dynamics*, 1999.
3. Kawakatsu Y., Yamamoto M., Kawaguchi J., Study on a Lunar Approach Strategy Tolerant of a Luanr Orbit Injection Failure, *Transactions of the Japan Society fro Aeronautical and Space Sciences Space Technology Japan*, Vol. 7, pp. 1-7, 2007.
4. Kawakatsu Y., Study on the Characteristics of Two-burn Translunar Trajectory, *Transactions of the Japan Society fro Aeronautical and Space Sciences Space Technology Japan*, Vol. 7, pp. 9-15, 2007.
5. Matsumoto S., Takizawa Y., Konishi H., et al., Lunar Transfer Orbit of SELENE, *Proceedings of 25th International Symposium on Space Technology and Science*, 2006.
6. Uesugi K., Matsuo H., Kawaguchi J., et al., Japanese First Double Lunar Swingby Mission "HITEN", *Acta Astronautica*, Vol. 25, pp. 347-355, 1991.
7. Belbruno E.A., Examples of the Nonlinear Dynamics of Ballistic Capture and Escape in the Earth-Moon System, AIAA 90-2896, 1990.
8. Miller J.K. and Belbruno E.A., A Method for the Construction of a Lunar Transfer Trajectory Using Ballistic Capture, AAS 91-100, 1991.
9. Yamakawa H., Kawaguchi J., Ishii N., et al., On Earth-Moon Transfer Trajectory with Gravitational Capture, *Advances in Astronautical Sciences*, Vol. 85, pp. 397-416, 1993.
10. Yamakawa H., Kawaguchi J., Ishii N., et al., A Numerical Study of Gravitational Capture Orbit in the Earth-Moon System, *Advances in Astronautical Sciences*, Vol. 79, pp. 1113-1132, 1992.